Dynamical Mode Coupling and Coherence in a Spin Hall Nano-Oscillator with Perpendicular Magnetic Anisotropy

Lina Chen, S. Urazhdin, Y.W. Du, and R.H. Liu

Phys. Rev. Applied **11**, 064038 — Published 17 June 2019

DOI: 10.1103/PhysRevApplied.11.064038

Dynamical mode coupling and coherence in spin Hall nano-oscillator with perpendicular magnetic anisotropy

Lina Chen[1], S. Urazhdin[2], Y.W. Du[1], and R. H. Liu[1,2]
[1]*National Laboratory of Solid State Microstructures, School of Physics and Collaborative Innovation Center of Advanced Microstructures, Nanjing University, Nanjing 210093, China*
[2]*Department of Physics, Emory University, Atlanta, GA 30322, USA.*

We experimentally study the dynamical modes excited by spin current in Spin Hall nano-oscillators based on the Pt/[Co/Ni] multilayers with perpendicular magnetic anisotropy. Both propagating spin wave and localized solitonic modes of the oscillation are achieved and controlled by varying the applied magnetic field and current. At room temperature, the generation linewidth broadening associated with mode hopping was observed at currents close to the transition between different modes and in the mode coexistence regimes. The mode hopping was suppressed at cryogenic temperatures, confirming that the coupling between modes is mediated by thermal magnon-mediated scattering. We also demonstrate that coherent single-mode oscillations with linewidth of 5 MHz can be achieved without applying an external magnetic field. Our results provide insight into the mechanisms controlling the dynamical coherence in nanomagnetic oscillators, and guidance for optimizing their applications in spin wave-based electronics.

PACS numbers: 75.78.-n, 75.75.-c, 75.30.Ds

I. INTRODUCTION

Spin transfer torque (STT), a torque exerted on the magnetization by the injected spin current, can counteract the natural dynamical damping in magnetic systems, resulting in magnetization reversal or sustained magnetization precession [1, 2]. Spin torque nano-oscillators (STNO), magnetic nanodevices based on the latter effect, can serve as nanoscale sources of microwave signals and spin waves, with possible applications in radio frequency electronics, spin wave-based electronic (magnonic) devices [3], and neuromorphic computing [4].

One of the main shortcomings of STNOs is their large microwave generation linewidth, motivating the ongoing experimental and theoretical studies of the mechanisms controlling the coherence of the dynamical magnetization states induced by STT. A theory based on the single-mode nonlinear oscillator approximation, developed by Slavin and co-workers, predicted that the dynamical coherence is determined by thermal fluctuations, whose effects are enhanced by the dynamical nonlinearity [5, 6]. However, real nanomagnetic systems are characterized by quasi-continuous spectrum of dynamical modes. As a result, mode coexistence, mode hopping, and/or periodic mode transitions are commonly observed in STNOs [7–12], significantly affecting the dynamical coherence.

In mode hopping, the magnetic system experiences random transitions between different dynamical states, with only a single mode excited at any given instant of time, indicating that the modes compete with each other and are generally incompatible. It is also possible for different modes to simultaneously coexist, which can be facilitated by the spatial separation of different modes, due, for example, to the current-induced Oersted field[10], the spatially inhomogeneous dipolar fields, and/or the spatial inhomogeneity of the magnetic properties of the system. To account for these observed effects, theories accounting for the multimodal behaviors of STNO have been recently developed [13, 14]. They provide insight into the mode coupling mechanisms essential for developing efficient microwave and spin-wave applications of STNOs. However, experimental verification of the mode coupling mechanisms for some of the most actively researched STNO types, such as described below, is still lacking.

Traditionally, STT applications utilized magnetic multilayers, where the current exerting STT on the "free" magnetic layer was spin-polarized by a separate spin-polarizing ferromagnet [15, 16]. More recently, an alternative, simpler and potentially more efficient approach has emerged [17–21], relying on spin currents produced by the spin Hall effect (SHE) [22], or on the spin-orbit torque (SOT) [23] directly exerted on the magnetic interface due to the Rashba effect [24]. These advancements have enabled the development of a novel type of STNO - the spin Hall nano-oscillator (SHNO) comprising a bilayer of an efficient spin Hall material and a ferromagnet (FM), without the need for a separate spin-polarizer [20, 21].

In SHNO, pure spin current generated by SHE in the materials with a large SHE, such as Pt or Ta, is locally injected into the adjacent FM layer, exciting either localized magnetization dynamics or propagating spin waves [25–32]. The potential advantages of SHNO, compared to the traditional multilayer STNOs, include simple planar structure enabling simultaneous fabrication and synchronization of multiple nano-oscillators [31], and their straightforward incorporation into magnonic structures [33]. Additionally, since SHNO do not require charge currents to flow through the magnetic layers, they are compatible with low-loss insulating magnetic materi-

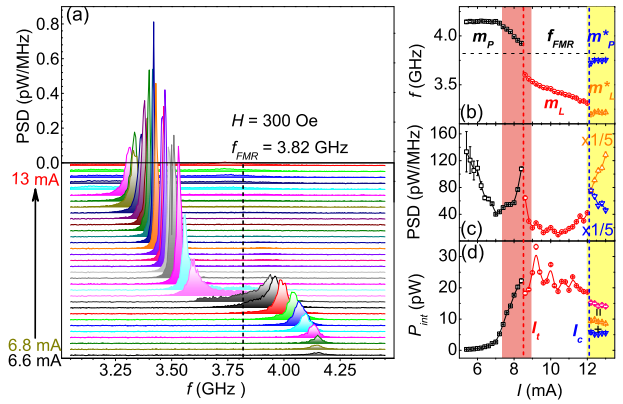

Figure 1: Dependence of the microwave generation characteristics of SHNO on current, at $H = 300$ Oe and $T = 295$ K. (a) Generation spectra, at current I varied between 6.6 mA and 13 mA in 0.2 mA steps. The dashed line is the ferromagnetic resonance (FMR) frequency f_{FMR} determined by the spin torque FMR (ST-FMR) technique. (b)-(d) Current dependence of the central generation frequency (b), full width at half maximum (FWHM) (c), and integral intensity (d) of the three dominant modes m_P, m_L and m_P^* defined in the text. The mode transition current I_t and the onset current I_C of mode coexistence are marked by the vertical dashed lines. The two shadowed regions mark the mode hopping (at 7.3 mA$<I<$ 8.9 mA) and mode coexistence (at $I >$ 12 mA) regimes. The spectral characteristics in (b)-(d) were extracted from the multipeak Lorentzian fitting of the spectra. At $I >$ 12 mA, the FWHMs of both the m_P^* and the m_L modes in panel (c) are divided by 5, as marked by $\times 1/5$. The symbols (+, ||) in panel (d) indicate the sum of the integral intensities P_{int} of the m_P^* and the m_L modes, giving the total intensity shown with diamonds.

als, enabling improved efficiency and reduced Joule heating [34]. Despite intense research of SHNO, the nature of transitions among different dynamical modes and their effects on the dynamical coherence remain largely unexplored.

Here, we report a systematic experimental study of the microwave generation characteristics of SHNO based on the FM film with perpendicular magnetic anisotropy (PMA). We analyze the dependence on the applied magnetic field, excitation current, and temperature, providing insight into the interactions among the dynamical modes, the effects of mode hopping and mode coexistence on the dynamical coherence and linewidth broadening of SHNO. Additionally, we demonstrate the possibility to achieve single-mode dynamics in the absence of applied magnetic field. Our experimental results provide a valuable test for the proposed theories of multimode dynamics, and suggest avenues for the control of spectral characteristics and generation power of SHNO for device applications.

II. EXPERIMENT AND RESULTS

A. Device fabrication and measurement setup

The studied device is based on a $Pt(5)/[Co(0.2)/Ni(0.3)]_6/SiO_2(3)$ magnetic multilayer film, deposited on the sapphire substrate by magnetron sputtering at room temperature. Thicknesses are given in nanometers. The magnetic multilayer film in the studied device has a well-defined perpendicular magnetic anisotropy (PMA), and exhibits bubble magnetic domains when a small field is applied in the plane of the film, as shown by our prior anomalous Hall effect (AHE) and anisotropic magnetoresistance (AMR) measurements for magnetic films with the same structure [29], and by other groups for similar films [35, 36]. The SHNO device consisted of the Pt/[Co/Ni] multilayer patterned into a disk with diameter of 4 μm, with two pointed Au(100) electrodes separated by a ∼100 nm gap fabricated on top of the disk, similar to the previously studied planar point contact SHNO [20, 29]. The microwave signals detected in our measurements were generated due to the AMR of the [Co/Ni] film, whose magnetization experienced precession induced by the spin current injected by the Pt layer. To enable microwave generation by spin current-induced magnetization dynamics, the spectroscopic measurements were performed with H tilted by 5° relative to the film plane, and forming an angle $\theta = 60°$ relative to the current direction. All the data shown below were obtained from the same device. The generality of the observed behaviors was confirmed by measurements on two additional devices with the same structure.

B. Spectral Characteristics of microwave generation

At room temperature $T = 295$ K, magnetization dynamics was observed above the auto-oscillation onset current I_{on}, at magnetic fields H ranging from 0 to almost 1.2 kOe, as illustrated in Figs. 1, 2. Figure 1 shows a representative dependence of the spectral characteristics on current I, obtained at $H = 300$ Oe. At the onset current $I_{on} = 5.4$ mA, the oscillation frequency $f = 4.15$ GHz was above the ferromagnetic resonance frequency $f_{FMR} = 3.82$ GHz determined by the spin torque ferromagnetic resonance (ST-FMR) technique [Fig. 1(a)] [37]. We note that since the oscillation frequency is above f_{FMR}, within the linear spectrum of the propagating spin-wave mode in the CoNi film, magnetization dynamics induced in the active device region by the local injection of spin current necessarily results in emission of spin waves at this frequency. Furthermore, since there is no magnetic barrier isolating the active region from the surrounding film, the coupling of the locally oscillating magnetization to spin waves must be strong. Thus, the current-induced dy-

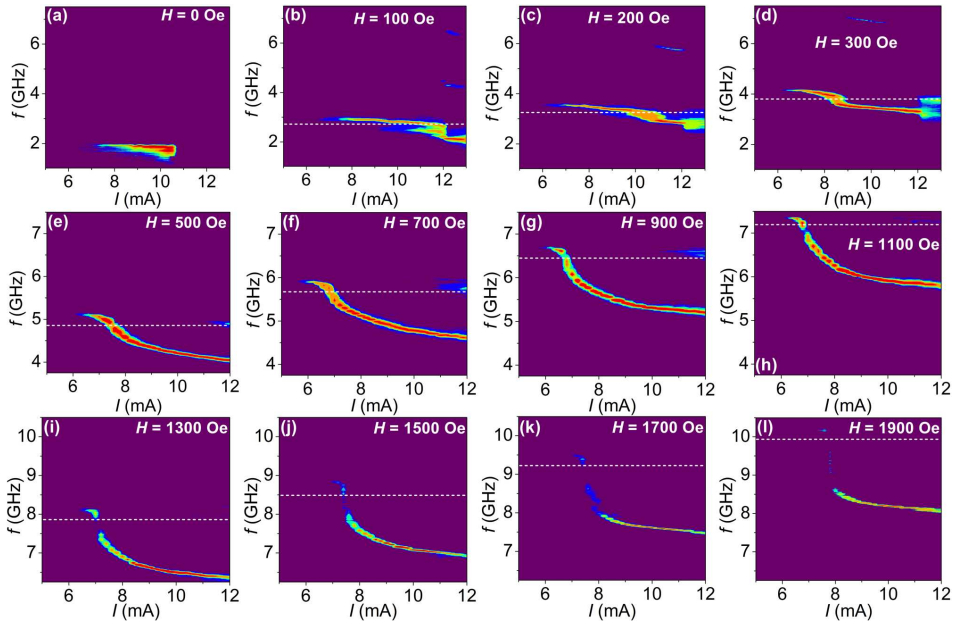

Figure 2: Pseudocolor maps of the dependence of the generated microwave spectra on current at $T = 295$ K, at magnetic field $H = 0$ Oe (a), 100 Oe (b), 200 Oe (c), 300 Oe (d), 500 Oe (e), 700 Oe (f), 900 Oe (g), 1100 Oe (h), 1300 Oe (i), 1500 Oe (j), 1700 Oe (k) and 1900 Oe (l). Dashed horizontal lines show the ferromagnetic resonance frequency f_{FMR} of the device determined by the ST-FMR technique.

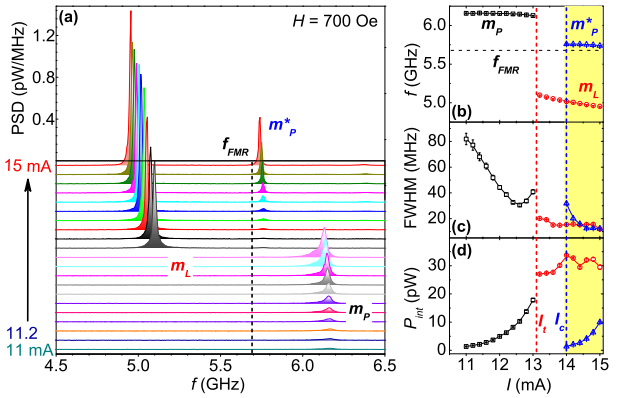

Figure 3: Dependence of the microwave generation characteristics on current, at $H = 700$ Oe and $T = 6$ K. (a) Generation spectra, at current I varied between 11 mA and 15 mA in 0.2 mA steps. The dashed line is f_{FMR} determined by the ST-FMR technique. (b)-(d) Current dependence of the central generation frequency (b), FWHM (c), and integral intensity (d) of the dominant modes labeled m_P, m_L and m_P^*. The mode transition current I_t and the onset current I_C of two-mode coexistence are marked by the vertical dashed lines. The shadowed region marks the mode coexistence regime. The spectral characteristics in (b)-(d) were extracted from the multipeak Lorentzian fitting of the spectra.

namics in this regime can be, to a good approximation, described as quasi-linear spin wave excitation by spin current, consistent with Slonczewski's theory of propagating spin wave emission by STNO with PMA free layer [1].

The oscillation peak exhibited a rapid increase of power, a very small blueshift, and a linear decrease of linewidth with increasing $I > I_{on}$ [Figs. 1(b-d)]. The linewidth decreased to a minimum value of 50 MHz at the same current $I_{p1} = 7.0$ mA as the maximum peak intensity, then started to increase at currents above $I = 7.2$ mA, accompanied by a large frequency redshift. Based on the nonlinear single mode auto-oscillator theory developed by Slavin and co-workers [6], the linewidth scales inversely with the power of the oscillation mode, which is determined by a combination of the auto-oscillation area and the amplitude of the auto-oscillation. In addition, the linewidth depends on the dynamical nonlinearity of the auto-oscillation, which mediates the coupling between the amplitude and the phase noise. The observed linewidth decrease at $I > I_{on}$, correlated with the rapid increase of generation power, is consistent with this theory. The linewidth increase observed at currents above 7.2 mA is correlated with the onset of a large frequency redshift, as expected due to the phase noise enhancement by coupling to the amplitude fluctuations [6].

At a current $I_t = 8.5$ mA, the oscillation frequency abruptly dropped to $f = 3.6$ GHz, below $f_{FMR} = 3.82$ GHz, and the linewidth also abruptly decreased. These behaviors can be attributed to the transition to a different auto-oscillation mode that does not belong to the linear spin-wave spectrum. In contrast to the propagating spin wave mode at small currents, in this regime the oscillation exhibited a strong red shift. Similar spectral features were previously observed in SHNO with in-

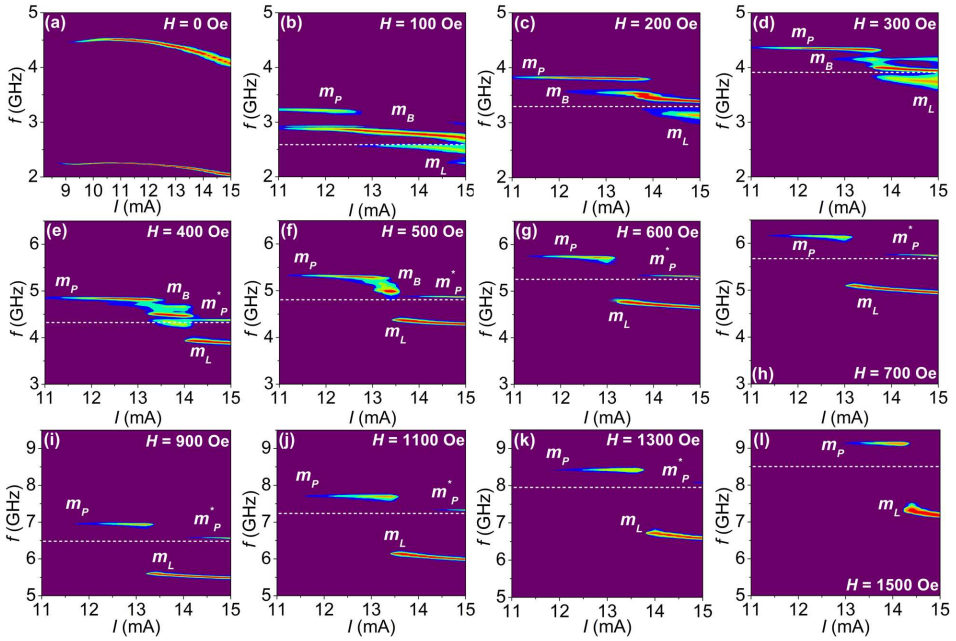

Figure 4: Pseudocolor maps of the dependence of the generated microwave spectra on current at $T = 6$ K, at the magnetic field $H = 0$ Oe (a), 100 Oe (b), 200 Oe (c), 300 Oe (d), 400 Oe (e), 500 Oe (f), 600 Oe (g), 700 Oe (h), 900 Oe (i), 1100 Oe (j), 1300 Oe (k) and 1500 Oe (l). Dashed horizontal lines show f_{FMR} determined by the ST-FMR technique. m_P, m_L and m_P^* mark the three distinct modes defined in the text.

plane magnetic anisotropy [20, 21] and the conventional multilayer STNO [10], and were identified with the nonlinear self-localized spin wave "bullet" mode [5]. We emphasize that the localized nature of this mode can be inferred directly from the fact that its frequency lies below f_{FMR}, implying that propagating dynamical states at this frequency are not allowed.

The strong redshift and linewidth broadening of the propagating mode, observed in the transition regime to the localized mode, marked by the red area in Fig. 1(b-d), can be attributed to the coupling between the two modes. The coupling, and consequently the mode broadening, is strongly suppressed at cryogenic temperatures, as discussed below [See Fig. 3]. With a further increase of current, an additional broad low-intensity peak emerges in the spectrum above $I_c = 12$ mA, at a frequency slightly below f_{FMR}. This is correlated with the decrease of intensity and broadening of the low-frequency "bullet" mode. The new peak can be attributed to the quasi-propagating mode that becomes weakly localized due to the Oersted field of the driving current, which is directed almost opposite to the applied field H. This interpretation, as well as the above analysis of the bullet and the propagating spin waves, is supported by detailed simulations for a similar PMA-based SHNO device reported in Ref. [29].

Multimodal dynamics such as observed in Fig. 1 at currents close to I_t and above I_c, is generally associated either with mode hopping or mode coexistence. The former is characterized by random transitions between mutually incompatible modes. Based on the abrupt crossover between qualitatively different dynamical behaviors at $I_t = 8.5$ mA, we can attribute this transition to mode hopping. Meanwhile, the behaviors at $I > I_c$ can be tentatively attributed to the emergence of mode coexistence. We provide further evidence for this interpretation below. We note that the linewidth doubles due to mode hopping near I_t, and increases by more than a factor of 5 due to the mutilmode excitation above I_c, demonstrating the importance of understanding the underlying mechanisms for the ability to control the spectral characteristics of SHNO.

Since the magnetic configuration of the system depends on both the driving current and the applied magnetic field H, further insight into the nature of the dynamical magnetization states is provided by analyzing the effects of varying H [Fig. 2]. At small fields $H < 100$ Oe, we observed a hysteresis of spectral characteristics consistent with magnetic history-dependent pinning of the magnetic bubbles on imperfections. In constrast to STNO with in-plane anisotropy, the studied SHNO device with PMA generated microwave signals at currents above 6.4 mA even in the absence of applied field, with an almost current-independent frequency $f = 1.8$ GHz [Fig. 2(a)]. The spectrum exhibited an asymmetric lineshape with a long low frequency tail, which is likely associated with the interplay between the current-induced dynamics and thermal hopping of magnetic bubbles in the vicinity of the active device region.

At 100 and 200 Oe, the propagating mode m_P was ex-

cited at small currents, while the localized "bullet" mode m_L appeared at larger currents, similarly to the behaviors at 300 Oe discussed above [Fig. 1]. An additional peak with two sidebands was observed between the m_P and m_L modes in the intermediate current range [more easily distinguished in the low-temperature data, Fig. 3 below]. Since this peak appeared in the same range of fields as the magnetic bubble domain state, it can be attributed to the dynamical bubble mode m_B. Both the bullet m_L and the dynamical bubble mode m_B consist of an inverted quasi-static core, with the magnetization dynamics occurring in the region separating this core from the extended magnetic film, as discussed in detail in Ref. [29]. At fields larger than 200 Oe, the magnetic bubble domain state was destroyed by the out-of-plane component of the field, and the dynamical bubble mode disappeared. Mode hopping at currents near I_t, and mode coexistence at currents above I_c were observed for all the measurement fields, although the intensity of the propagating mode m_P^* decreased with increasing field, as shown in Fig. 2(e-l). The reduced mode coupling with increasing field is due to the increasing frequency separation between the propagating modes and the localized "bullet" mode, as well as the gradual suppression of the propagating modes.

According to the theory of multimodal dynamics [12, 14], mode coupling among the dominant modes plays an essential role in the mode hopping and mode coexistance. The coupling can originate from several different linear and non-linear mechanisms, including thermal magnon-mediated scattering arising from the interaction between the dominant modes and the bath of thermally excited magnons, direct exchange interaction between modes, and/or their dipolar interaction. The first mechanism is associated with the existence of a bath of thermally excited magnons, which facilitate conservative four-magnons scattering involving two thermal magnons coupled to the two dominant modes. In the studied devices, thermal magnon populations are affected not only by temperature, but also by the current due to the current-driven spin torque and spin pumping effects. In addition, Joule heating of the active device area also contributes to thermal magnon excitation.

To identify the mode coupling mechanisms in the SHNO, spectroscopic measurements were repeated at a cryogenic temperature $T = 6$ K, where thermal effects are significantly reduced. In the studied range of driving currents, the temperature of the active device area was 50-60 K, as estimated by comparing the R *vs* I and the R *vs* T curves used in Ref. [21]. Figure 3 shows the dependence of spectral characteristics on I, at a representative field H = 700 Oe. The high-frequency propagating mode m_p was observed at small current, followed by an abrupt transition to the low-frequency localized "bullet" mode at $I_t = 13$ mA, with another high frequency propagating mode appearing near f_{FMR} above $I_c = 14$ m A. These behaviors are qualitatively similar to those observed at T =295 K. However, in contrast to the room-temperature data shown in Fig. 2, the current-dependent spectra of the three dominant modes - high frequency propagating mode m_P, intermediate-frequency "bubble skyrmion" soliton mode m_B, and the low-frequency localized "bullet" mode m_L, observed in certain field ranges [Fig. 4] - exhibit clearly distinct spectral characteristics, not noticeably affected by the presence of another mode, or proximity to the transition between modes. These behaviors indicate that mode coupling causing mode hopping near the mode transition in the studied SHNO is strongly suppressed, suggesting that thermal magnon-mediated scattering, rather than direct interactions between the modes, is the mechanism of mode coupling in the studied SHNO.

We note that thermal effects also play a significant, but different, role in the magnetization dynamics observed in the absence of applied field [Figs. 2(a), 4(a)]. At 6 K, the spectrum exhibits a narrow oscillation peak at 2.25 GHz, with the minimum linewidth $FWHM = 5$ MHz, without the low-frequency tail observed at 295 K. Moreover, the presence of a well-pronounced second harmonic of the oscillation clearly demonstrates that a large amplitude of the oscillation is achieved. These results support our interpretation of room-temperature broadening in terms of the interplay between oscillation and thermal fluctuations of the magnetic bubbles, which become suppressed at cryogenic temperatures.

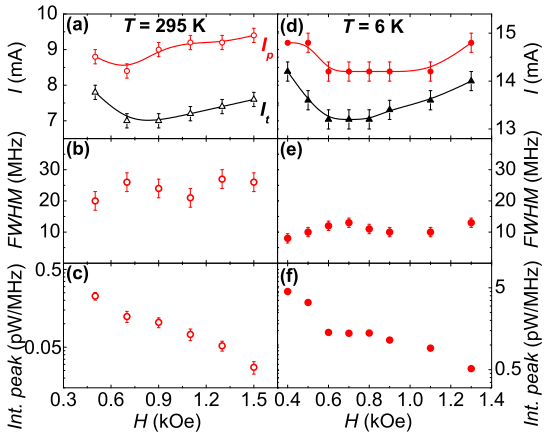

Figure 5: Dependence of the microwave generation characteristics on field H at 295 K and 6 K. (a)-(d) The characteristic currents I_p, and I_t defined in the text, (b)-(e) FWHM, (c)-(f) peak intensity at currents I_p.

To gain further insight into the thermal effects on the generation linewidth of SHNO, we focus on the single-mode excitation regime. We exclude the data obtained at $H \leq 300$ Oe, since these results are affected by the complex dynamics of bubbles present at small fields. Next, in analyzing the dependence on the magnetic field, we eliminate the possible artifacts coming from the depen-

dence of characteristic currents on field, by focusing on the field-dependent current value I_p corresponding to the minimum linewidth of the localized bullet mode, which coincides with the highest peak power density. As the data in Figs. 5(a) and (d) show, the current I_p remains far away from the mode transition current I_t. Therefore, the spectral characteristics observed at I_p are to a good approximation determined by the direct effects of thermal fluctuations on the single-mode dynamics. The characteristic currents I_t and I_p exhibited a similar overall field dependence, with a broad minimum around $H \simeq 700$ Oe both at 6 K and 295 K [Fig. 5(a) and (d)], similar to the prior observations for SHNOs with in-plane magnetization [20, 38]. While the maximum peak power generated at I_p exhibited an exponential decrease with increasing field [Fig. 5(c) and (f)], the minimum linewidth of 25±5 MHz at room temperature was almost field-independent, and only about 2 times larger than 10±3 MHz at 6 K [Fig. 5(b) and (e)], indicating that the broadening is associated not only with the effects of temperature on thermal magnon [39], but also with the large effect on the incoherent magnon population produced by the spin current [32].

We note that in addition to the thermal effects on the mode transition and coexistence discussed above, the dynamical behaviors of the studied magnetic nanodevices depend on several temperature-dependent contributions, including the magnetization, magnetic anisotropy, Gilbert damping, the spin diffusion length, the resistivity of both the CoNi multilayer and Pt, and the spin Hall angle of the latter. These temperature-dependent parameters have been extensively discussed in the literature. The cumulative effects of their temperature dependence on the spin-current induced dynamics can be expected to amount to a modest rescaling of the characteristic oscillation currents and magnetic fields controlling the observed dynamical regimes, as well as the characteristic frequencies. This general expectation is supported by the comparison of the data acquired at 295 K and 6 K. For example, the oscillation onset current at modest fields increases from about 6 mA at room temperature to 11 mA at 6 K, and the dynamical bubble state remains stable in a larger field range at 6 K (0 - 500 Oe) than that at room temperature (0 - 200 Oe) due to a larger PMA and coercivity at low temperature. Nevertheless, the observed mode structure and the overall dependence on current and field remain consistent.

III. CONCLUSION

To summarize, we demonstrated that spin Hall nano-oscillator based on the Pt/[Co/Ni] multilayer with PMA exhibits several distinct dynamical regimes, which can be achieved by varying the applied oblique field and current. The propagating spin wave mode is observed at small currents, transitioning to the localized "bullet" soliton mode, similar to that observed in spin-torque oscillators with in-plane magnetic anisotropy. Besides the propagating and the "bullet" modes, a "bubble skyrmion" soliton mode correlated with the magnetic bubble state at small fields is also observed, enabling coherent auto-oscillations in the absence of the applied field. At room temperature, mode hopping and multimode coexistence, observed over certain current ranges, degrade the spectral characteristics. These effects are remarkably suppressed at a cryogenic temperature, demonstrating that the thermal magnon-mediated scattering mechanism dominates the coupling between dynamical modes. Our results suggest a practical approach not only to controlling the microwave spectral properties of spin Hall nano-oscillators for rf-applications by suppressing the thermal coupling induced mode hopping, but also to utilizing the nonlinear coupling among well-defined interacting modes to develop of the novel neuromorphic computation schemes for artificial intelligence (AI), based on the arrays of coupled nanomagnetic oscillators[40, 41].

ACKNOWLEDGMENTS

L.N.C, Y.W.D and R.H.L are supported by the National Key Research and Development Program of China (2016YFA0300803), National Natural Science Foundation of China (No.11774150), Applied Basic Research Programs of Science and Technology Commission Foundation of Jiangsu Province (BK20170627), and the Open Research Fund of Jiangsu Provincial Key Laboratory for Nanotechnology. S.U. acknowledges support from NSF grant Nos. ECCS-1804198 and DMR-1504449.

[1] J. C. Slonczewski, Current-driven excitation of magnetic multilayers,J. Magn. Magn. Mater. **159**, L1 (1996).
[2] L. Berger, Emission of spin waves by a magnetic multilayer traversed by a current, Phys. Rev. B **54**, 9353 (1996).
[3] V. V. Kruglyak1, S. O. Demokritov, and D. Grundler, Magnonics, J. Phys. D: Appl. Phys. 43 264001(2010).
[4] J. Torrejon, M. Riou, F. A. Araujo, S. Tsunegi, G. Khalsa, D. Querlioz, P. Bortolotti, V. Cros, K. Yakushiji, A. Fukushima, H. Kubota, S. Yuasa, M. D. Stiles, and J. Grollier, Neuromorphic computing with nanoscale spintronic oscillators, Nature **547**, 428 (2017).
[5] A. Slavin, and V. Tiberkevich, Spin wave mode excited by spin-polarized current in a magnetic nanocontact is a standing self-localized wave bullet, Physical review letters 95, 237201 (2005).
[6] J. V. Kim, V. Tiberkevich, and A. N. Slavin, Generation linewidth of an auto-oscillator with a nonlinear frequency shift: spin-torque nano-oscillator, Physical review letters 100, 017207 (2008).

[7] P. K. Muduli, O. G. Heinonen, and J. Åkerman, Temperature dependence of linewidth in nanocontact based spin torque oscillators: Effect of multiple oscillatory modes, Physical Review B 86, 174408(2012).

[8] P. Bortolotti, A. Dussaux, J. Grollier, V. Cros, A. Fukushima, H. Kubota, K. Yakushiji, S. Yuasa, K. Ando, and A. Fert, Temperature dependence of microwave voltage emission associated to spin-transfer induced vortex oscillation in magnetic tunnel junction, Applied Physics Letters 100, 042408 (2012).

[9] J. F. Sierra, M. Quinsat, F. Garcia-Sanchez, U. Ebels, I. Joumard, A. S. Jenkins, B. Dieny, M. C. Cyrille, A. Zeltser, and J. A. Katine, Influence of thermal fluctuations on the emission linewidth in MgO-based spin transfer oscillators, Applied Physics Letters 101, 062407 (2012).

[10] R. K. Dumas, E. Iacocca, S. Bonetti, S. R. Sani, S. M. Mohseni, A. Eklund, J. Persson, O. Heinonen, and J. Åkerman, Spin-wave-mode coexistence on the nanoscale: a consequence of the Oersted-field-induced asymmetric energy landscape, Physical review letters 110, 257202 (2013).

[11] R. Sharma, P. Dürrenfeld, E. Iacocca, O. G. Heinonen, J. Åkerman, and P. K. Muduli, Mode-hopping mechanism generating colored noise in a magnetic tunnel junction based spin torque oscillator, Applied Physics Letters 105, 132404 (2014).

[12] E. Iacocca, P. Dürrenfeld, O. Heinonen, J. Åkerman, and R. K. Dumas, Mode-coupling mechanisms in nanocontact spin-torque oscillators, Physical Review B 91, 104405(2015).

[13] E. Iacocca, O. Heinonen, P. K. Muduli, and J. Åkerman, Generation linewidth of mode-hopping spin torque oscillators, Physical Review B 89, 054402(2014).

[14] S. S. L. Zhang, E. Iacocca, and O. Heinonen, Tunable Mode Coupling in Nanocontact Spin-Torque Oscillators, Physical Review Applied 8, 014034(2017).

[15] M. Tsoi, A.G.M. Jansen, J. Bass, W.C. Chiang, M. Seck, V. Tsoi, and P. Wyder, Excitation of a Magnetic Multilayer by an Electric Current, Phys. Rev. Lett. **80**, 4281 (1998).

[16] J.A. Katine, F.J. Albert, R.A. Buhrman, E.B. Myers, and D.C. Ralph, Current-Driven Magnetization Reversal and Spin-Wave Excitations in Co /Cu/Co Pillars,Phys. Rev. Lett. **84**, 3149 (2000).

[17] I. M. Miron, G. Gaudin, S. Auffret, B. Rodmacq, A. Schuhl, S. Pizzini, J. Vogel, and P. Gambardella, Current-driven spin torque induced by the Rashba effect in a ferromagnetic metal layer, Nature Materials **9**, 230 (2010).

[18] L. Q. Liu, O. J. Lee, T. J. Gudmundsen, D. C. Ralph, and R. A. Buhrman, Current-Induced Switching of Perpendicularly Magnetized Magnetic Layers Using Spin Torque from the Spin Hall Effect, Phys. Rev. Lett. **109**, 096602 (2012).

[19] R. H. Liu, W. L. Lim, and S. Urazhdin, Control of current-induced spin-orbit effects in a ferromagnetic heterostructure by electric field, Phys. Rev. B **89**, 220409(R) (2014).

[20] V.E. Demidov, S. Urazhdin, H. Ulrichs, V. Tiberkevich, A. Slavin, D. Baither, G. Schmitz, and S. O. Demokritov, Magnetic nano-oscillator driven by pure spin current, Nat. Mater. **11**, 1028 (2012).

[21] R.H. Liu, W.L. Lim, and S. Urazhdin, Spectral Characteristics of the Microwave Emission by the Spin Hall Nano-Oscillator, Phys. Rev. Lett. **110**, 147601 (2013)

[22] M. I. Dyakonov and V. I. Perel, Possibility of Orienting Electron Spins with Current, Sov. Phys. JETP Lett **13**, 467 (1971).

[23] A. Manchon, and S. Zhang, Theory of Spin Torque Due to Spin-Orbit Coupling, Phys. Rev. B. **79**, 094422 (2009).

[24] Y. A. Bychkov and E. I. Rashba, Oscillatory effects and the magnetic susceptibility of carriers in inversion layers, Journal of Physics C **17**, 6039 (1984).

[25] V. E. Demidov, S. Urazhdin, A. Zholud, A. V. Sadovnikov, and S. O. Demokritov, Nanoconstriction-based spin-Hall nano-oscillator, Applied Physics Letters 105, 172410 (2014).

[26] Z. Duan, A. Smith, L. Yang, B. Youngblood, J. Lindner, V. E. Demidov, S. O. Demokritov, and I. N. Krivorotov, Nanowire spin torque oscillator driven by spin orbit torques, Nature communications **5**, 5616 (2014).

[27] A. Zholud, and S. Urazhdin, Microwave generation by spin Hall nanooscillators with nanopatterned spin injector, Applied Physics Letters **105**, 112404 (2014).

[28] H. Ulrichs, V. E. Demidov, and S. O. Demokritov, Micromagnetic study of auto-oscillation modes in spin-Hall nano-oscillators, Applied Physics Letters **104**, 042407 (2014).

[29] R. H. Liu, W. L. Lim, and S. Urazhdin, Dynamical Skyrmion State in a Spin Current Nano-Oscillator with Perpendicular Magnetic Anisotropy, Physics Review Letter **114**, 137201 (2015).

[30] H. Mazraati, S. Chung, A. Houshang, M. Dvornik, L. Piazza, F. Qejvanaj, S. Jiang, T. Q. Le, J. Weissenrieder, and J. Akerman, Low operational current spin Hall nano-oscillators based on NiFe/W bilayers, Applied Physics Letters **109**, 242402 (2016).

[31] A. A. Awad, P. Dürrenfeld, A. Houshang, M. Dvornik, E. Iacocca, R. K. Dumas, and J. Åkerman, Long-range mutual synchronization of spin Hall nano-oscillators, Nature Physics **13**, 292 (2016).

[32] S. Urazhdin, V. E. Demidov, R. Cao, B. Divinskiy, V. Tyberkevych, A. Slavin, A. B. Rinkevich, and S. O. Demokritov, Mutual synchronization of nano-oscillators driven by pure spin current, Applied Physics Letters **109**, 162402 (2016).

[33] V. E. Demidov, S. Urazhdin, G. de Loubens, O. Klein, V. Cros, A. Anane, and S. O. Demokritov, Magnetization oscillations and waves driven by pure spin currents, Physics Reports **673**, 1-31 (2017).

[34] V. E. Demidov, M. Evelt, V. Bessonov, S. O. Demokritov, J. L. Prieto, M. Munoz, J. Ben Youssef, V. V. Naletov, G. de Loubens, O. Klein, M. Collet, P. Bortolotti, V. Cros, and A. Anane, Direct observation of dynamic modes excited in a magnetic insulator by pure spin current, Scientific reports **6**, 32781 (2016).

[35] G. H. O. Daalderop, P. J. Kelly, and F. J. A. den Broeder, Prediction and Confirmation of Perpendicular Magnetic Anisotropy in Co/Ni Multilayers, Phys. Rev. Lett. **68**, 682 (1992).

[36] G. Chen, T. P. Ma, A. T. N'Diaye, H. Y. Kwon, C. Won, Y. Z. Wu, and A. K. Schmid, Tailoring the chirality of magnetic domain walls by interface engineering, Nat. Commun. **4**, 2671 (2013).

[37] O. Mosendz, J. E. Pearson, F.Y. Fradin, G.E.W. Bauer, S.D. Bader, and A. Hoffmann, Quantifying Spin Hall Angles from Spin Pumping: Experiments and Theory, Phys.

Rev. Lett. **104**, 046601 (2010).
[38] R. H. Liu, Lina Chen, S. Urazhdin, and Y.W. Du, Control of spectral characteristics of spin-current auto-oscillator by electric field, Physical Review Applied **8**, 021001 (2017).
[39] J.-V. Kim, Stochastic theory of spin-transfer oscillator linewidths, Physical Review B **73**, 174412 (2006)
[40] D. Vodenicarevic, N. Locatelli, F. A.Araujo, J.Grollier, and D.Querlioz, A nanotechnology-ready computing scheme based on a weakly coupled oscillator network, Sci. Rep. **7**, 44772 (2017).
[41] M. Romera, P. Talatchian, S. Tsunegi, F. Abreu Araujo, V. Cros, P. Bortolotti, J. Trastoy, K. Yakushiji, A. Fukushima, H. Kubota, S. Yuasa, M. Ernoult, D. Vodenicarevic, T. Hirtzlin, N. Locatelli, D. Querlioz, J. Grollier, Vowel recognition with four coupled spin-torque nano-oscillators, Nature **563**, 230-234 (2018).